# Supplemental Information

## Ternary Morphology Facilitated Thick-Film Organic Solar Cell

Jiangquan Mai[1], Tsz Ki Lau[1], Ting Xiao[2], Chun-Jen Su[3], U-ser Jeng[3], Ni Zhao[2], Xudong Xiao[1], Xinhui Lu[1]*

1. Department of Physics, Chinese University of Hong Kong, New Territories,

   Hong Kong. E-mail: xhlu@phy.cuhk.edu.hk

2. Department of Electronic Engineering, Chinese University of Hong Kong, New

   Territories, Hong Kong.

3. National Synchrotron Radiation Research Center, 101 Hsin-Ann Road, Hsinchu

   Science Park, Hsinchu, Taiwan,
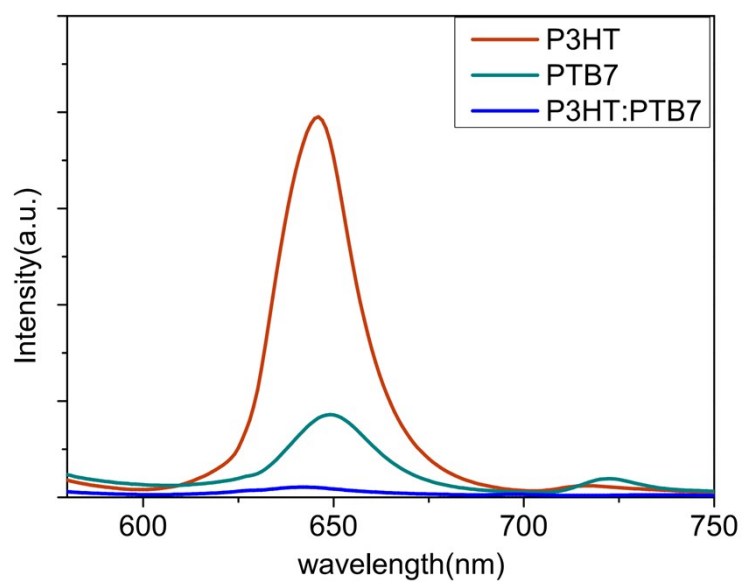
Fig. S1. Photoluminescence emission spectrums of pristine P3HT, pristine PTB7 and P3HT/PTB7 blend film. All the films were excited with 510 nm wavelength incident light.
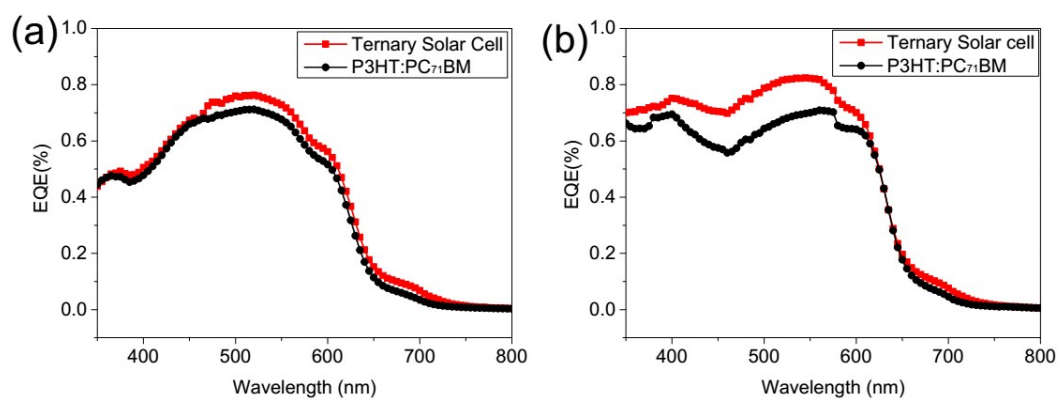
Fig. S2. External quantum efficiency (EQE) of ternary P3HT:PTB7:PC71BM (16:1:17.5) and binary P3HT:PC71BM (1:1) solar cells with (a) ~100 nm active layer; (b) ~200 nm active layer;
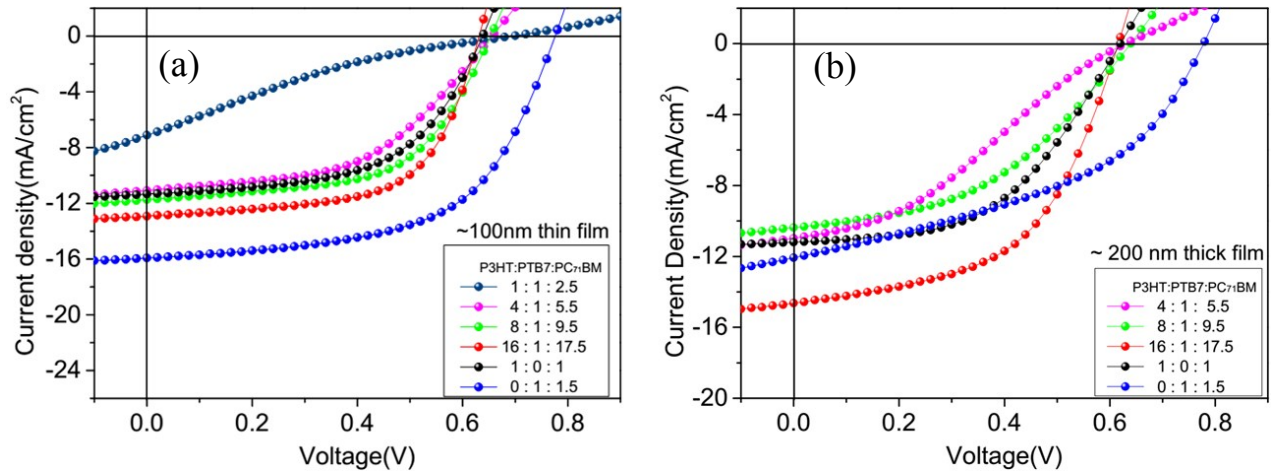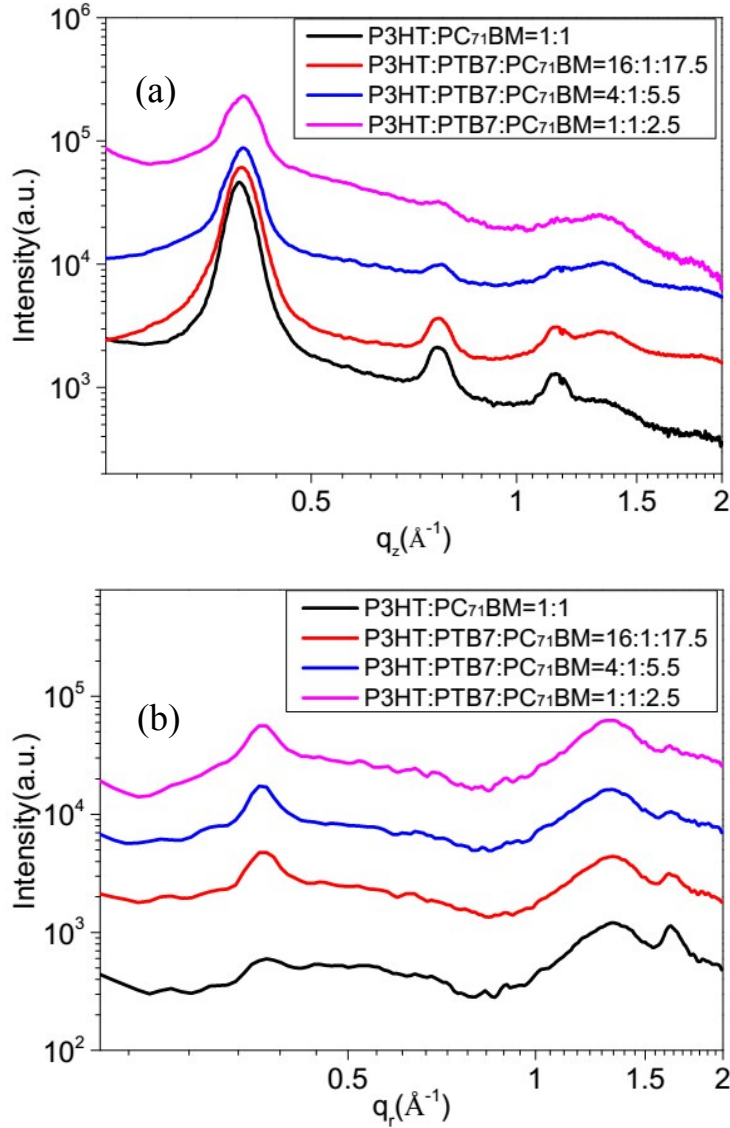
Fig. S3. J-V curves of ternary solar cells with different mass ratios: (a) ~100 nm active layer and (b) ~200 nm active layer. In ternary films, the ratios of P3HT:$PC_{71}BM$=1:1 and PTB7:$PC_{71}BM$=1:1.5 are fixed. The optimized mass ratio is P3HT:PTB7:$PC_{71}BM$=16:1:17.5.
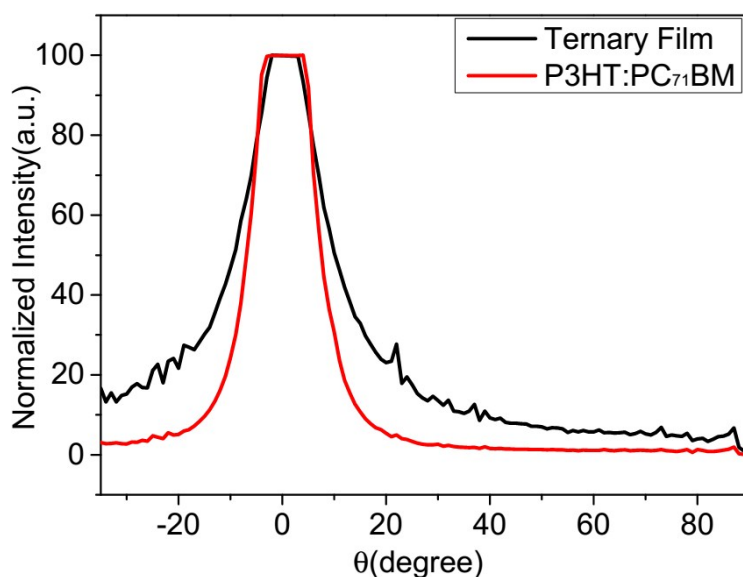
Fig. S4. GIWAXS intensity integration of BHJ films of different mass ratios along (a) q_z axis (normal to surface) and (b) q_r axis (parallel to surface) respectively (displaced for clarity).

From the q_z intensity integration (Fig. S4a), we found that the intensity of P3HT lamellae peak decreased when the mass ratio of PTB7 increased, suggesting that excessive sensitizer would undermine the crystallization process of P3HT and

destroyed the pristine bulk heterojunction matrix. Probably the reason is that the chains of P3HT and PTB7 may entangle and interact with each other in the ternary solution, hence the PTB7 chains would prevent P3HT from forming a highly order structure though it was annealed after spin coating. Fig. S4b shows the intensity integration along q_r which represents the in-plane structure of the thin films. The π-π stacking peak (010) become weaker in ternary cell but the lamellar peak (100) become stronger. It suggests that though the crystallinity of P3HT decreases in ternary film, part of the molecular packing turns to face-on structure, but the order of this face-on structure does not enhance with the increase of PTB7 concentration.


Fig. S5. GIWAXS intensity integration of P3HT (100) peak as function of its polar angle. Fitted by Lorentz distribution function, the Full width at half maximum is 9.15° in ternary film, and 5.03° in P3HT:PC$_{71}$BM film. It indicated the order of P3HT edge-on structure decreased in ternary film.
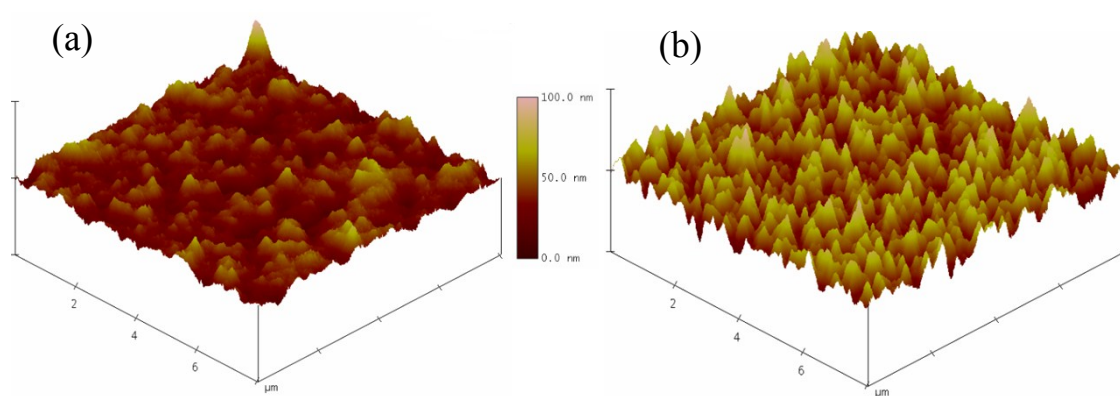
Fig. S6. 3D atomic force microscope (AFM) images of top surface of bulk heterojunction films, (a) P3HT:PC$_{71}$BM binary film, (b) P3HT:PTB7:PC$_{71}$BM ternary film. To study the surface morphology of thin films, we also conducted the atomic force microscope (AFM) measurement.

Fig. S6 is tapping mode AFM images which give comparison between top surface of the P3HT:PC$_{71}$BM binary film (a) and P3H:PTB7:PC$_{71}$BM(16:1:17.5) ternary film (b). It is observed that the surface roughness of ternary film is much larger than binary film, which is calculated in root mean square (rms) is 6.1 nm (binary) and 10.3 nm (ternary). The rougher top surface in ternary film probably resulted from the formation of a more ordered structure in the BHJ film. However, using the surface area calculation function of our AFM program, the surface area in ternary film was found to be only 0.71% more than the binary film, which should have minor contribution to the observed device performance improvement.
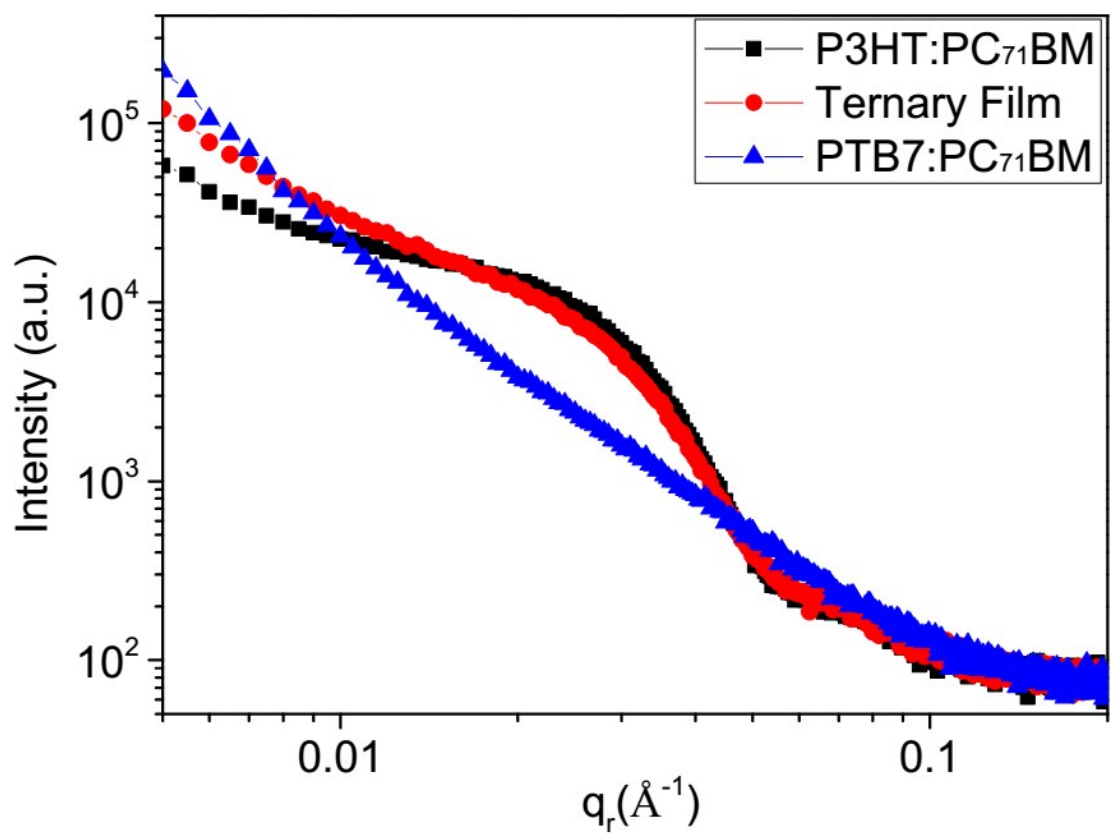
Fig. S7 GISAXS profile of P3HT:PC71BM, PTB7:PC71BM binary films and

P3HT:PTB7:PC71BM (16:1:17.5) ternary film